Spatio-Spectral Gamut Mapping and Separation

Sepideh Samadzadegan

Technische Universität Darmstadt, Fraunhoferstr. 5, 64283 Darmstadt, Germany
E-mail: sepideh.samadzadegan@gris.informatik.tu-darmstadt.de

Philipp Urban▲

Fraunhofer Institute for Computer Graphics Research IGD, Fraunhoferstr. 5, 64283 Darmstadt, Germany

Abstract. *Spectral printing aims to achieve an illuminant-invariant match between the original and the reproduction. Due to limited printer spectral gamuts, an errorless spectral reproduction is mostly impossible, and spectral gamut mapping is required to reduce perceptual errors. The recently proposed paramer-mismatch-based spectral gamut mapping (PMSGM) strategy minimizes such errors. However, due to its pixel-wise processing, it may result in severely different tonal values for spectrally similar adjacent pixels, causing unwanted edges (banding) in the final printout. While the addition of some noise to the a* and b* channels of the colorimetric (e.g., CIELAB) image—rendered for the first illuminant—prior to gamut mapping solves the banding problem, it adversely increases the image graininess. In this article, the authors combine the PMSGM strategy with subsequent spectral separation, considering the spatial neighborhood within the tonal-value space and the illuminant-dependent perceptual spaces to directly compute tonal values. Their results show significant improvements to the PMSGM method in terms of avoiding banding artifacts.* © 2015 Society for Imaging Science and Technology.
[DOI: 10.2352/J.ImagingSci.Technol.2015.59.4.040402]

INTRODUCTION

The quality of hardcopy reproduction is often adversely affected by limitations of printing systems, particularly the colorimetric gamut. It is defined by all colors printable by a device considering specific media, inks and viewing conditions, i.e., an illuminant and observer. Since conventional printing systems utilize four colorants (CMYK), the colorimetric gamut is usually restricted in the secondary colors (red, green and blue). Nowadays, there are multichannel printers using more than four colorants (e.g., CMYKRGB) in order to expand the printer gamut. Although by utilizing these kinds of printing systems, the reproduction of more colors is possible, out-of-gamut colors must still be mapped into the printer gamut by employing colorimetric gamut mapping algorithms (GMAs).[1] These methods commonly have the aim of minimizing the perceived difference between the original input image and the final print for one considered illuminant.

A byproduct of such multichannel printers is a high colorimetric redundancy, i.e., that different colorant com-binations might result in the same or nearly the same color for a specified viewing condition. We may utilize the colorimetric redundancy for improving the print quality for other illuminants. This is referred to as *spectral reproduction*, where the reproduction is adjusted to match the original image under various (ideally all) illuminants.

The spectral reproduction workflow consists of spectral gamut mapping, spectral separation, ink limitation and halftoning. In this article, we are focusing on the first two parts of this workflow. More information about ink limitation and halftoning can be found in Refs. 2, 3.

The spectral printer gamut is defined as the set of all printable reflectances reproducible by a printing system (consisting of the printer, the halftone used, the inks employed and the media). Thus, it is independent of the illuminant. Since the spectral gamut of any existing printing system is much smaller than the gamut spanned by all natural reflectances, it is rather unlikely that an arbitrary reflectance lies inside a printer's spectral gamut. Hence, spectral gamut mapping methods are required to map given out-of-gamut reflectances into the spectral gamut of the printer. The resulting printable spectra are inputs to a spectral separation method that computes appropriate colorant combinations for their reproduction. For this, a spectral printer model must be inverted, which is usually performed by solving a constrained optimization problem.[4,5]

In general, spectral gamut mapping methods can be categorized into three main groups based on their operational space. These three categories are

- spectral space-based approaches,
- perceptual and spectral space-based approaches, and
- multi-illuminant perceptual space-based approaches.

Spectral GMAs are more complex than colorimetric GMAs because they must consider more than the three colorimetric dimensions. For spectral space-based approaches (first category), access to the spectral gamut boundaries is required. Different approaches have been proposed for accessing the colorimetric gamut boundaries,[6,7] while only a few have been published so far to access the boundaries of a spectral printer gamut. For instance, Bakke et al.[8] applied principal component analysis (PCA) on spectral data in order to reduce the high dimensionality of the spectral space. They used the convex hull in this lower dimensional space

to describe the boundary of the spectral gamut. Spectral gamut mapping was fully performed in the spectral space by mapping out-of-gamut reflectances into the spectral gamut of the printer along a line towards the gamut center.

Spectral gamut mapping algorithms belonging to the first category are based on spectral metrics. A drawback associated with these metrics is that they are not very well correlated with human perception. Therefore, even small computed spectral differences may lead to large perceptual errors for distinct viewing conditions.

There are other approaches that operate in perceptual and spectral spaces (second category). For instance, in an approach proposed by Rosen and Derhak,[9] a colorimetric–spectral hybrid interim connection space (ICS) called LabPQR was used. The first three dimensions (Lab) represent CIELAB coordinates—considering a specific illuminant—while the last three (PQR) are coordinates of the so-called metameric black space. For each CIELAB value inside the colorimetric gamut, a nested gamut representing the metameric redundancy is defined using the PQR dimensions. The spectral gamut mapping is performed by transforming any input reflectance into this hybrid space using two stages: a colorimetric one and a spectral one. In the colorimetric part, a traditional colorimetric gamut mapping is performed and a PQR nested gamut is defined for each resulting CIELAB value. In the spectral part, gamut mapping is conducted for the PQR values that are outside the nested gamuts. Even though spectral errors are reduced by this approach, this method cannot ensure small colorimetric errors for illuminants other than the specified one.

Another approach, proposed by Tsutsumi et al.,[10] is also based on the LabPQR hybrid space. The main difference from the previous method is that in this approach both the colorimetric and the spectral parts are combined into a single objective function. Colorant combinations are chosen by minimizing the weighted sum of the normalized Euclidean distances computed in the PQR spectral space and the CIEDE2000 colorimetric differences calculated in the CIELAB space.

In addition to these approaches, which are based on low-dimensional and at least partly spectral ICSs, the spectral GMAs of the third category operate only within multiple perceptual spaces defined for different viewing conditions.[11–13] In these approaches, a hierarchy of application-dependent illuminants sorted from the most to the least important one is considered under which the reproduction is adjusted to the original input. In this way, color-difference formulas (e.g., CIEDE2000) can be used to compute relevant errors for the considered viewing conditions, which have a much higher correlation with human color-difference perception than spectral RMS differences.

It is worth mentioning that there are some other approaches for spectral reproduction related to halftoning not considered in this article.[14]

The fundamental of the proposed method in this article is based on the paramer-mismatch-based spectral gamut

mapping (PMSGM)[12] framework, which belongs to the third category. We therefore will give a more detailed explanation of the PMSGM framework. The results of the PMSGM method show a high colorimetric accuracy under the considered illuminants but suffer from banding artifacts. In this article, we show how these banding artifacts can be minimized by combining the PMSGM framework with spectral separation considering the spatial neighborhood within the tonal-value space.

TERMINOLOGY

In this article, we use nearly the same terminologies and notations as used in Refs. 12, 13.

CIEXYZ tristimulus values—considering $r(\lambda)$ as the surface reflectance and $I(\lambda)$ as the spectral power distribution (SPD) of an illuminant, the CIEXYZ tristimulus values are obtained via the following equation:

$$X(I, r) = \frac{100}{\int_\Lambda \bar{y}(\lambda) I(\lambda)\, d\lambda} \int_\Lambda \begin{bmatrix} \bar{x}(\lambda) \\ \bar{y}(\lambda) \\ \bar{z}(\lambda) \end{bmatrix} I(\lambda) r(\lambda)\, d\lambda, \quad (1)$$

where $\Lambda = [380, 730]$ nm is the visible wavelength range, and the CIE color matching functions (CMFs) are denoted by $\bar{x}$, $\bar{y}$ and $\bar{z}$.

Color space transformations—although the proposed method does not rely on any specific color space, it is recommended to utilize a perceptually uniform and hue-linear color space such as LAB2000HL,[15] which is a trichromatic opponent color space similar to CIELAB. The transformation from the CIELAB color space to LAB2000HL coordinates as well as the inverse transformation are performed via lookup tables (nodes of the lookup tables represent a direct sampling of the transformation and intermediate values are interpolated from neighboring nodes). The supplementary material of the LAB2000HL article[15] contains MATLAB scripts encoding the lookup tables and color space transformations. In this article, the direct transformation from CIEXYZ to LAB2000HL color space is denoted by $L : \text{CIEXYZ} \mapsto \text{LAB2000HL}$, which is a concatenation of the CIEXYZ to CIELAB and CIELAB to LAB2000HL transformation. It should be mentioned that Euclidean distances in LAB2000HL color space are almost equal to corresponding CIEDE2000 distances in CIELAB. Hence, for calculating color differences in LAB2000HL we use the 2-norm.

Metamer definition—two reflectances $r_1(\lambda)$ and $r_2(\lambda)$ are called metamers for a specific illuminant $I(\lambda)$ if

$$\|L(X(I, r_1)) - L(X(I, r_2))\|_2 = 0. \quad (2)$$

This means that the corresponding tristimuli match perfectly.

Paramer definition—two reflectances $r_1(\lambda)$ and $r_2(\lambda)$ are called paramers for a specific illuminant $I(\lambda)$ if

$$\|L(X(I, r_1)) - L(X(I, r_2))\|_2 \leq D, \quad (3)$$

where D is the just noticeable color difference (JND). This definition is similar that of Urban and Berns.[12] It means that colors of paramers for the specified illuminant are not exactly equal but indistinguishable.

Spectral printer gamut—is defined as the set of all printable reflectances reproducible by a printing system (consisting of the printer, the halftone used, the inks employed and the media). Thus it is independent of the illuminant. We denote the spectral printer gamut with the symbol $\mathcal{G}$.

Metameric or colorimetric printer gamut—is the set of all colors reproducible by a printing system for a specific illuminant $I(\lambda)$. It is denoted with the symbol G and specified by the following transformation:

$$G(I, \mathcal{G}) = L(X(I, \mathcal{G})). \qquad (4)$$

THE PARAMER-MISMATCH-BASED SPECTRAL GAMUT MAPPING (PMSGM) FRAMEWORK

Because the approach proposed in this article is based on the PMSGM framework,[12] we give a detailed overview of its concept and implementation for a CMYKRGB printer.

PMSGM Overview

The objective of PMSGM is to achieve a similar reproduction quality to a traditional metameric reproduction for one selected illuminant and a superior quality (with respect to colorimetric errors) under other considered illuminants. For this purpose, any metameric gamut mapping method used in traditional metameric reproduction can be included into the PMSGM framework. The approach consists of subsequent gamut mapping transformations within multiple color spaces defined for a hierarchy of the considered illuminants sorted from the most to the least important one.

PMSGM as well as the method proposed in this article do not require access to the spectral gamut boundaries.

The input to the framework is the spectral image (R) and the sorted list of illuminants $I_1, \ldots, I_n$. In the first step, colorimetric images (e.g., represented in CIELAB/LAB2000HL) are computed from the spectral image for all illuminants in the list. In the second step, the colorimetric image rendered for the first (most important) illuminant is mapped into the colorimetric gamut of the printer $G(I_1, \mathcal{G})$ using a traditional gamut mapping method denoted by Γ_{Trad}.[1] Here, spatial gamut mapping algorithms[16,17] can also be used for obtaining the highest quality.

Due to the printer's colorimetric redundancies, the resulting in-gamut color of a pixel p_0 can be reproduced by a set of different colorant combinations $\rho(p_0)$ with a non-noticeable error (below JND) for the first illuminant. Thus, the printed reflectances corresponding to $\rho(p_0)$ are paramers for I_1. We denote $\rho(p_0)$ as the *parameric set* for p_0 and I_1.

For the second illuminant I_2, these paramers may result in distinguishable colors defining a so-called *paramer-mismatch gamut*. The original color of pixel p_0 under I_2 must be mapped into this paramer-mismatch gamut to not (noticeably) alter the gamut mapping under I_1. This mapping can be performed by minimizing the color difference for optimizing colorimetric accuracy under I_2. The concept can be extended to adjust the reproduction to all considered illuminants by exploiting the printer's colorimetric redundancy. The result is a colorant combination satisfying colorimetric criterion across the hierarchical set of illuminants, resulting in a color which agrees with the result of the employed metameric gamut mapping up to a JND for the most important illuminant. This procedure is performed for all image pixels, resulting in the *separation image S* containing the colorant combinations to control the printer.

Figure 1 illustrates the PMSGM framework considering two illuminants. The colorant, spectral and colorimetric spaces as well as an example of a device- and pixel-dependent paramer-mismatch gamut are also shown in this figure.

Shortcomings of PMSGM

Urban and Berns[12] proposed a pixel-wise implementation of PMSGM by performing the gamut mapping transformations described above independently from the pixel neighborhood. Even though this ensures a high colorimetric quality for each pixel, it may result in unwanted *banding artifacts* caused by introducing edges in the resulting separation image in areas where the original spectral image is smooth. The avoidance of such banding is possible by adding noise to the a⋆ and b⋆ channels of the CIELAB image rendered for the first illuminant, at the expense of increasing *graininess*. Samadzadegan and Urban[13] proposed an approach aimed at avoiding both banding and graininess, which they called the *spatially resolved joint spectral gamut mapping and separation* (SGMS) method. It traverses all image pixels and uses a cost function for selecting a colorant combination from the actual parameric set $\rho(p_0)$, taking into account colorimetric criteria (as in Ref. 12) and the colorant combination of already processed pixels in a local pixel neighborhood. Even though this approach can drastically minimize banding, it introduces other artifacts (called *smearing*) due to the directional traversal scheme (top-left to bottom-right) and the accumulation of spatial errors in the traversal direction. Figure 2 shows examples of structural artifacts introduced in one channel of the separation image by the approaches described above. In this article, we propose an enhancement of the SGMS method by a modified cost function and an initialization step, avoiding banding and smearing artifacts and reducing graininess.

METHODOLOGY

Step 1: Rendering the Spectral Image

Consider that we have n illuminants $I_1(\lambda), \ldots, I_n(\lambda)$ sorted from the most to the least important one for a specific application. In the first step, we render the spectral image R, with the size of $N \times M$ pixels, into a colorimetric (e.g., LAB2000HL) image for each of the abovementioned illuminants and a CIE standard observer. This process yields n LAB2000HL images (see Figure 6, Step 1). Each pixel of the
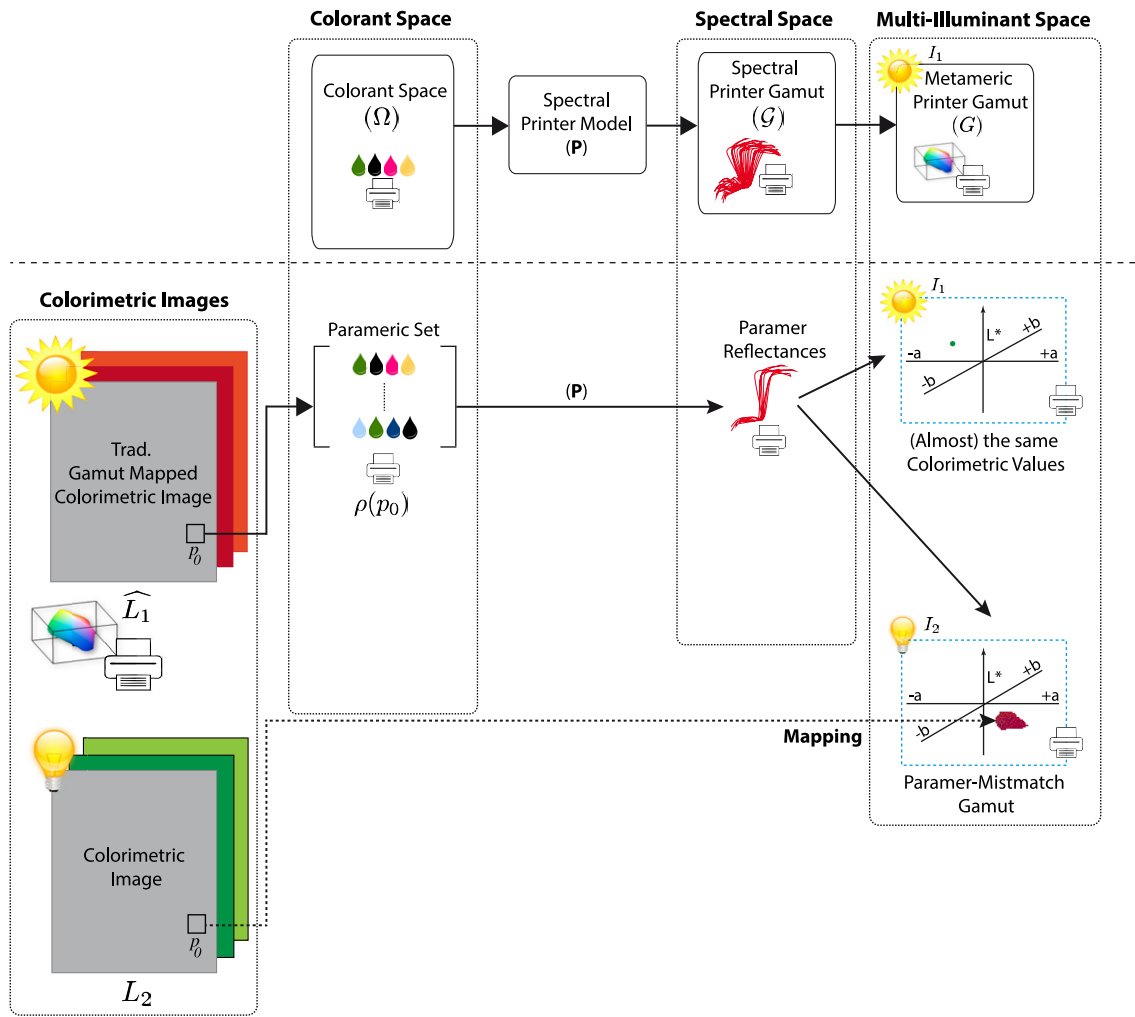
Figure 1. Schematic representation of the PMSGM framework—the fundamental of the proposed method in this article—in a multi-illuminant structure considering two illuminants.
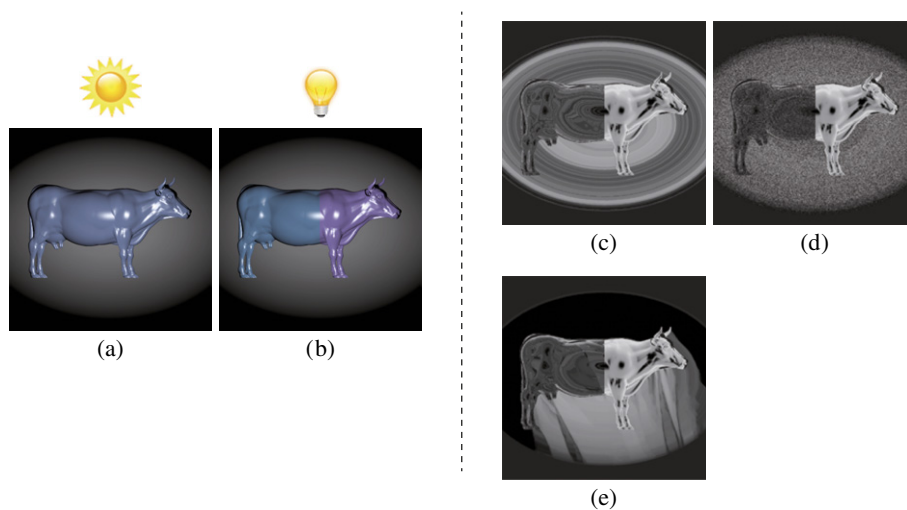

Figure 2. A cut-out of the METACOW image[18] rendered for (a) CIED65 and (b) CIEA illuminants. The separation images generated by the PMSGM[12] method (without and with the addition of a small amount of noise) and the SGMS[13] approach are represented in (c), (d) and (e), showing the banding, graininess and smearing artifacts, respectively. It should be noted that for the sake of brevity, only one channel out of the seven-channel separation image (CMYKRGB) is shown, where the increased amount of colorant combinations (per image pixel) is represented via a gradient from white (no ink) to black (100% ink).

spectral image is rendered into n LAB2000HL pixels via

$$l_{x,y}(i) = L(X(I_i, r_{x,y})), \qquad (5)$$

where $i = 1, \ldots, n$ is the illuminant index and x, y is the pixel position. The ith LAB2000HL image is defined by

$$L_i : \begin{cases} \underline{N} \times \underline{M} \to \text{LAB2000HL}, \\ (x, y) \to l_{x,y}(i), \end{cases} \qquad (6)$$

where $\underline{N} = \{1, \ldots, N\}$ and $\underline{M} = \{1, \ldots, M\}$.

Step 2: Initialization by Averaging
In this step, we compute an average LAB2000HL value for all pixels of each LAB2000HL image rendered in the previous step. The following equation represents the averaged LAB2000HL value for each image:

$$l_{\text{Avg}}(i) = \frac{\sum_{x=1}^{N} \sum_{y=1}^{M} l_{x,y}(i)}{N \times M}, \qquad (7)$$

where $i = 1, \ldots, n$ represents the illuminant index. Using the PMSGM method[12] explained previously, one colorant combination is computed from these n LAB2000HL colors. An *initial separation image* S with the size of $N \times M$ pixels is created by assigning this colorant combination to each pixel.

Step 3: Traditional Gamut Mapping
Since our goal is to be as good as the metameric reproduction for the first illuminant (which is the most important one) and to be better than the metameric reproduction for the second and subsequent illuminants, we apply a traditional colorimetric GMA (Γ_{Trad}) for the first LAB2000HL image L_1 rendered for the first illuminant I_1:

$$\Gamma_{\text{Trad}}[G(I_1, \mathcal{G})] : L_1 \mapsto \widehat{L}_1. \qquad (8)$$

The input of this transformation is the metameric printer gamut $G(I_1, \mathcal{G})$ for the first illuminant. The main aim of employing the traditional gamut mapping is to generate another image $\widehat{L}_1$ which is inside the metameric gamut of the printer $G(I_1, \mathcal{G})$ and has the smallest perceptual color difference from the original image L_1. It should be noted that any colorimetric GMA is applicable, including spatial GMAs.

Step 4: Cost Function
To compute the final separation image, our method traverses the image from the first top-left to the final bottom-right pixel and computes a colorant combination for each image pixel. Since the final separation image is obtained by updating the initial separation image, it is also denoted by S.

Unlike the pixel-wise PMSGM[12] method, this approach considers both the *colorimetric* and the *spatial* content of the rendered colorimetric images. The spatial part takes into account the direct neighbors of each image pixel in a 3×3 spatial window. Figure 3 is a schematic representation of traversing the image together with the actual pixel p_0 and its direct neighbors $p_1, \ldots, p_8$. It should be noted that for
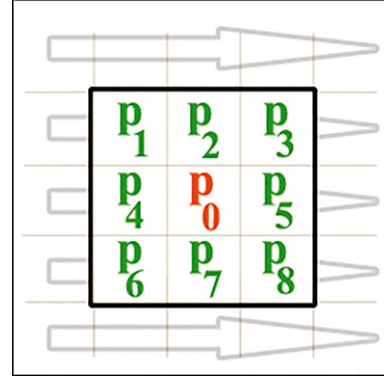

Figure 3. Traversing the image from the first top-left to the final bottom-right pixel. The actual under-process pixel is denoted by p_0, which has up to eight direct neighbors ($p_1, \ldots, p_8$) in a 3×3 spatial window.

border pixels the number of adjacent pixel neighbors is less than eight.

To compute the final colorant combination $S(p_0)$ for each pixel p_0, the following optimization problem has to be solved:

$$S(p_0) = \arg\min_{x \in \rho(p_0)} F_{\text{cost}}(x), \qquad (9)$$

where S is the separation image, F_{cost} is a cost function which is explained in Eq. (11) and below, and $\rho(p_0)$ is the set of parameric colorant combinations for pixel p_0 considering the first illuminant I_1, i.e.,

$$\rho(p_0) = \{x \in \Omega \mid \|P_1(x) - \widehat{L}_1(p_0)\|_2 \leq D\}, \qquad (10)$$

where Ω is the printer's colorant space, $P_1(x)$ is the color prediction of the printout under illuminant I_1 given the colorant combination x, i.e., $P_1(x) = L(X(I_1, P(x)))$ for a spectral printer model P (e.g., P could be the widely used cellular-Yule–Nielsen–spectral-Neugebauer (CYNSN) model[19–23]), $\widehat{L}_1(p_0)$ is the LAB2000HL color at pixel position p_0 extracted from the gamut mapped LAB2000HL image for the first illuminant I_1, and D is the JND.

The cost function $F_{\text{cost}} : \Omega \mapsto [0, 1]$ includes *colorimetric* as well as *spatial* criteria and is defined as follows:

$$F_{\text{cost}}(x) = 1 - f_{\text{col}}(x) f_{\text{spatial}}(x), \qquad (11)$$

where x is a colorant combination, and f_{col} and f_{spatial} are the colorimetric and spatial parts of the cost function used to make a trade-off between the colorimetric and spatial accuracy. These parts are explained in detail in Step 4.1: Colorimetric Part and Step 4.2: Spatial Part. It should be noted that f_{spatial} (and thus F_{cost}) depends on the pixel p_0 and its direct neighbors. This is not indicated by additional parameters for the sake of brevity.

Step 4.1: Colorimetric Part
In the colorimetric part, the color differences between the predicted LAB2000HL values $P_i(x) = L(X(I_i, P(x)))$, $x \in \rho(p_0)$, and the colorimetric values extracted from the

rendered LAB2000HL images are taken into account:

$$f_{\text{col}}(x) = \prod_{i=2}^{n} \exp\left(-\frac{1}{\sigma_1}\|P_i(x) - L_i(p_0)\|_2\right), \qquad (12)$$

where $i = 2, \ldots, n$ is the illuminant index, σ_1 is a weighting parameter and $L_i(p_0)$ is the LAB2000HL value at pixel position p_0 under illuminant I_i. As previously mentioned, the L_1 image was already mapped into the colorimetric gamut (G) of the printer defined for the first illuminant I_1; hence, in this equation, only the second and subsequent illuminants (denoted by index $i = 2, \ldots, n$) are considered.

If the reflectance of pixel p_0 lies within the spectral gamut of the printer $\mathcal{G}$, the color differences across all illuminants will be 0 and the result of the colorimetric part of the cost function will be 1. For color differences larger than 0, the colorimetric part becomes smaller than 1 but still remains positive. It should be noted that the 2-norm in LAB2000HL is almost equal to the CIEDE2000 differences of corresponding colors in CIELAB.

Step 4.2: Spatial Part
To compute the spatial part of the cost function, all direct neighbors of an image pixel in a 3×3 spatial window are considered (see Fig. 3). Moreover, their corresponding colorant combinations are used. The initialization step in Step 2: Initialization by Averaging ensures that a colorant combination is assigned to each image pixel. These colorant combinations are updated during the traversal process. Equation (13) represents the spatial part of the cost function:

$$f_{\text{spatial}}(x) = \exp\left(-\frac{1}{\wp}\left\|\sum_{j \in B} \omega(p_j)S(p_j) - x\right\|_2\right), \qquad (13)$$

where x is a colorant combination, B is the set of adjacent neighbors for pixel p_0, $S(p_j), j \in B$, is the actual colorant combination for pixel p_j, $\omega(p_j) \geq 0, j \in B$, is a *spatial weight* computed by Eq. (14) for pixel p_j, and $\wp$ is a *weight* defined in Eq. (15).

The main aim of weighting the colorant combinations of neighboring pixels is edge preservation, which is adopted from bilateral filtering. Instead of spatial distances and range differences we use color differences for all considered illuminants. These weights are calculated based on the degree of color deviations as follows:

$$\omega(p) = \frac{\prod_{i=1}^{n} \exp\left(-\frac{1}{\sigma_2}\|L_i(p_0) - L_i(p)\|_2\right)}{\sum_{j \in B} \prod_{i=1}^{n} \exp\left(-\frac{1}{\sigma_2}\|L_i(p_0) - L_i(p_j)\|_2\right)}, \qquad (14)$$

where σ_2 is a weighting parameter.

If the color differences between the actual image pixel $L_i(p_0)$ and its neighbor $L_i(p)$ considering all illuminants ($i = 1, \ldots, n$) are small, then the associated weight is larger than in the case where there is a large color difference (i.e., a sharp edge). The denominator ensures that all weights sum up to 1, i.e., $\sum_{j \in B} \omega(p_j) = 1$. The spatial part $f_{\text{spatial}}(x)$

becomes 1 if the weighted average of the neighboring pixels' colorant combinations is equal to x and decreases quickly if the weighted average deviates from x. Incorporated into the optimization shown in Eq. (9), this forces the separation image to mimic the local spatial correlation of the original image, i.e., avoiding banding artifacts but preserving (also metameric) edges.

A dominating f_{spatial} would preserve the local spatial correlation of the original image at the expense of potential large colorimetric errors under illuminants $I_2, \ldots, I_n$. If f_{col} is dominating, the separation image possesses banding artifacts as in the pixel-wise PMSGM approach. To balance the contributions of the colorimetric and spatial functions in the overall cost function to achieve high color accuracy without banding artifacts, we require a weighting parameter that adapts to the original image content. In smooth image regions the spatial part must dominate to avoid banding. In image regions with low spatial correlation (edges), the colorimetric part must dominate to increase the colorimetric accuracy for the considered illuminants. For this purpose, the parameter $\wp$ adapts to the image content as follows:

$$\wp = \sigma_3 + \min_{j \in B}\left(\sum_{i=1}^{n}(\|L_i(p_0) - L_i(p_j)\|_2)^2\right), \qquad (15)$$

where σ_3 is a weighting parameter.

The magnitude of $\wp$ controls the contribution of f_{spatial}. The larger $\wp$ is, the less the contribution of f_{spatial} is in the cost function. If p_0 is surrounded by at least one pixel with a similar color across illuminants (a smooth image region), $\wp \approx \sigma_3$ and f_{spatial} has maximum impact on the cost function to avoid banding (note that the weights within f_{spatial} decrease the impact of the other non-similar surrounding pixels). In high-frequency regions, such as edges, $\wp$ may become much larger than σ_3 and the impact of f_{spatial} diminishes. This allows the separation to start with a high colorimetric accuracy across illuminants if the traversal passes an edge.

After traversing each pixel of the image and selecting an optimal colorant combination by minimizing the cost function in Eq. (9), the final separation image S is computed. This image is then further processed (ink limited and halftoned) to control the printer.

Remarks
Additional (Optional) Step 1: Initialization by Segmentation
Instead of initializing the separation image by averaging (Step 2: Initialization by Averaging), segmentation can be used for improving the colorimetric accuracy—mostly apparent at metameric/parameric edges (edges appearing under one illuminant but invisible under another illuminant). We have not found these kinds of edges in natural images, but we cannot exclude such cases in general, and artificial images such as the METACOW[18] image include them.

As an example, the segmentation process can be applied on the rendered LAB2000HL images using a color-based segmentation method (e.g., k-means clustering[24]). After

(a) (b)
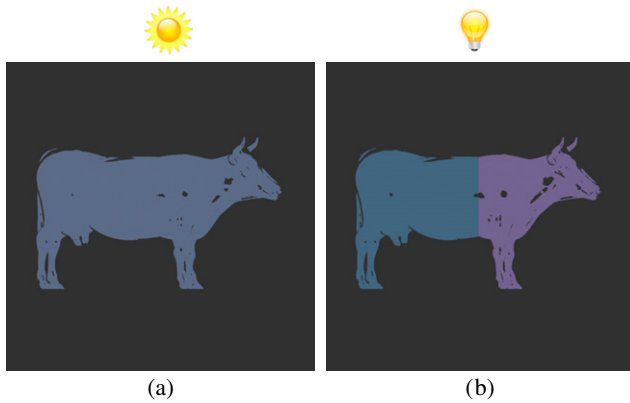
Figure 4. The segmented and cluster-wise averaged LAB2000HL images of a cut-out of the METACOW[18] image for (a) CIED65 and (b) CIEA illuminants. A color-based segmentation method using *k*-means clustering[24] was utilized for the segmentation, resulting in two and three clusters for CIED65 and CIEA illuminants, respectively.

performing the segmentation process, an averaged LAB2000HL value of all pixels within each cluster is calculated.

The initial colorant combinations and consequently the *initial separation image S* are then computed by applying the PMSGM[12] method on the segmented and cluster-wise averaged LAB2000HL images.

The colorant combination from the parameric set with the highest colorimetric accuracy will likely be more similar to the weighted average of surrounding colorant combinations (used in f_{spatial}) if the initialization is performed by averaging the actual cluster rather than the whole image. Therefore, such colorant combinations are more likely to be selected by the optimization, which improves the colorimetric accuracy. In this way, metameric/parameric edges between clusters are better preserved while avoiding banding within the cluster.

It should be mentioned that it is not necessary to segment the LAB2000HL images—rendered for different illuminants—into the same number of clusters.

We applied this scenario on a cut-out of the META-COW[18] image where the rendered LAB2000HL images for CIED65 and CIEA illuminants were segmented into two and three clusters, respectively. The result of this segmentation process as well as cluster-wise averaging is illustrated in Figure 4.

For automatic detection of images with metameric/parameric edges for which initialization by segmentation is useful, various strategies are thinkable, e.g., performing edge detection on the LAB2000HL images rendered for each of the considered illuminants and then applying a pixel-wise xor-operation on the resulting binary images. If the resulting binary image contains edges, they are metameric/parameric edges and a segmentation can be performed. A further investigation of segmentation strategies for the purpose of spectral gamut mapping would be another article and should be left for future research.

Additional (Optional) Step 2: Noise Addition
This step is optional and might be useful for artificial noise-free images such as the METACOW image.[18] The addition of a small amount of noise into the image rendered for the first illuminant adds high-frequency components into the final separation image. These high-frequency components break up remaining unwanted low-frequency patterns (banding) in the separation image.

To illustrate this, we added zero-mean Gaussian noise with a standard deviation of 2.55 to all channels of the noise-free CIELAB METACOW[18] image, rendered for the first illuminant (CIED65) prior to gamut mapping. The black channel of the resulting separation image is shown in Figure 8(e). This amount of added noise does not visibly affect the graininess of the printout.

Figures 5 and 6 illustrate the proposed approach.

EXPERIMENTS
Printing System and Implementation
We used an HP Designjet Z3100 printer controlled by the ONYX ProductionHouse RIP Version 7. The CMYKRGB standard inks and HP Premium Instant-dry Gloss Photo Paper were used.

Similarly to related work,[4,12,13] we restricted the number of overprints per pixel to four: a combination of the black ink (K) together with three other inks selected from CMYRGB. We assume that most of the colors within the spectral gamut of the CMYKRGB printer are covered by these colorant combinations.

For modeling the printer, we employed 20 cellular-Yule–Nielsen–spectral-Neugebauer (CYNSN) models,[19–23] for all possible four ink overprint combinations including the black colorant: CMYK, CMKR, CMKG, CMKB, CYKR, CYKG, CYKB, CKRG, CKRB, CKGB, MYKR, MYKG, MYKB, MKRG, MKRB, MKGB, YKRG, YKRB, YKGB and KRGB.

The four-dimensional colorant space of each of these 20 printer submodels was sampled in steps of 1%, which leads to 10^8 colorant combinations for each submodel. In total, $20 \times 10^8 = 2$ billion colorant combinations were considered to define the colorant space Ω.

The spectral printer gamut $\mathcal{G}$ was specified implicitly via the predicted reflectances from the printer control values (colorant combinations) as the result of applying the aforementioned spectral printer submodels.

To compute the parameric sets (see Eq. (10)), the LAB2000HL color space[15] was divided into cubes having approximately 0.4 CIEDE2000 side length, which is below the JND for office viewing conditions. In order to have quick access to these parameric sets, all of the colorant combinations for which the printer model LAB2000HL predictions for the first illuminant fell into the same cube were stored in separate lists. The optimization in Eq. (9)—used for separation—was simply performed by evaluating the cost function for each element of the list and choosing the colorant combination with the smallest cost function value.

```
Rendering the spectral image into LAB2000HL images                              Step 1
IF (no metameric/parameric edge) THEN
    Averaging each LAB2000HL image into a single LAB2000HL value                Step 2
    Initialization of the separation image by averaging
ELSE
    Segmentation of each LAB2000HL image and then averaging within each cluster   Optional Step 1
    Initialization of the separation image by segmentation and averaging
END IF
IF (completely noise-free images) THEN
    Adding a small amount of noise to the image rendered for the first illuminant   Optional Step 2
END IF
Traditional gamut mapping for the first illuminant                              Step 3
Applying the cost function (colorimetric and spatial parts)                     Step 4
```

Figure 5. Pseudocode implementation of the method.
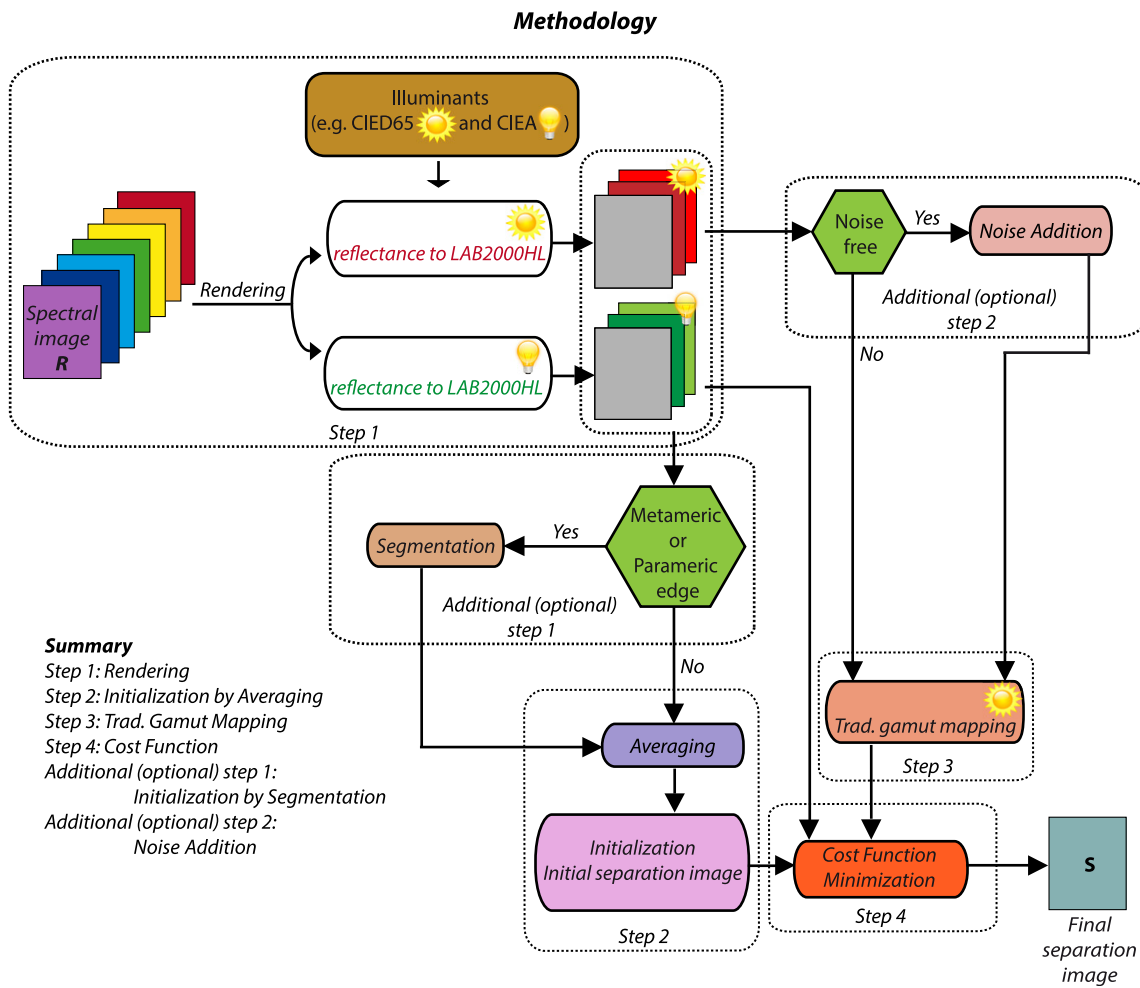

Figure 6. A block diagram representing the proposed methodology in an overall view.

Test Images

In order to test the proposed method and adjust the weighting parameters (σ_1, σ_2 and σ_3) (see Eqs. (12), (14) and (15)) of the cost function, the following 11 spectral images were considered as inputs to the framework:

- the METACOW[18] image (containing metameric edges),
- eight spectral images of natural scenes taken from the Foster database,[25]
- two paintings.

A Canon EOS 5D Mark III camera was used for capturing the printed images. No white balancing or chromatic adaptation was used for displaying the pictures.

Adjustment of the Cost Function's Parameters

The weighting parameters (σ_1, σ_2 and σ_3) of the proposed cost function (see Eqs. (12), (14) and (15)) are constant and

Table I. The weighting parameters of the proposed method together with their adjusted values.

Parameter	Value
σ_1	3
σ_2	2
σ_3	9

do not depend on the resolution. If the separation image contains discontinuities where the original image is smooth, banding artifacts are produced by subsequent halftoning (abrupt change in dot placement at the discontinuities produces banding). Independently of the resolution, the optimization must avoid such discontinuities to the largest extent (note that we use only a 3×3 window to account for spatial neighborhood) and similarly provide a high colorimetric accuracy.

We selected the parameters as conservatively as possible, by manually adjusting them on the noise-free METACOW[18] image with the aim of preserving the metameric edges and avoiding banding—we controlled the outcome by visually inspecting the channels of the separation image. We are aware of the fact that this approach is suboptimal.

Table I lists the weighting parameters together with their adjusted values.

RESULTS AND DISCUSSION

We tested the proposed method using 11 spectral images: eight natural scenes from the Foster database,[25] two paintings, and the METACOW image.[18]

In the following, we selected two images from this set to illustrate the performance of our method (METACOW[18] and the House image[25]). It should be noted that for the other images, our approach, the PMSGM and the SGMS method show the same quality deviations as illustrated by these two example images. Figures 7 and 8 show a comparison between the separation images of a natural scene[25] (House image) and a cut-out of the METACOW[18] image generated by these approaches: the PMSGM[12] method (a) without and (b) with the addition of zero-mean Gaussian noise with a standard deviation of 2.55 to all channels of the CIELAB image rendered for the first illuminant (CIED65) prior to gamut mapping, (c) the SGMS[13] approach and (d) the proposed method. The (a), (b) and (c) separation images represent the banding, graininess and smearing artifacts, respectively, while (d) demonstrates the reduction of all of these artifacts, leading to better separation results.

In Fig. 8, (e) represents a separation image generated by the proposed method and the application of both optional steps (segmentation of LAB2000HL images into two and three clusters for CIED65 and CIEA illuminants, respectively, and addition of a small amount of noise).

For the sake of brevity only one channel out of the seven-channel (CMYKRGB) separation images is shown in Figs. 7 and 8, where the amount of utilized ink (per image pixel) is represented by a gradient of white (no ink) and black (100% ink) neutral colors.

It should be noted that although the application of the PMSGM[12] method and the addition of a small amount of noise removes the banding artifacts, it adversely increases the image graininess (see (b) in Figs. 7 and 8).

Figure 9 illustrates cut-outs of captured images from spectral prints, generated by the separations shown in Fig. 7. The capture was performed under the two illuminants CIED65 (first row) and CIEA (second row). The banding, graininess and smearing artifacts are visible in (a) to (c), while (d) shows the improved reproduction.

Moreover, the separation images shown in Fig. 8 (a) and (e) were also sent to the printer. In Figure 11, the middle and bottom rows show the captured images under CIED65 (left) and CIEA (right) illuminants.

In order to show the advantage of spectral printing, the same cut-out of the METACOW[18] image was also printed, but with an ICC-based metameric workflow. The top row of Fig. 11 shows these captured images for the illuminants CIED65 and CIEA. As can be seen, the rear and front of the cow have the same color also under the CIEA illuminant and the metameric edge is gone using metameric reproduction. Spectral printing (PMSGM and the proposed method) creates reproductions that mimic the colors of the original (see Fig. 2(a) and (b)), particularly the color deviations between the cow's rear and front under illuminant CIEA.

For the natural images and paintings used in our evaluation we have not seen such clear colorimetric improvements of our method compared with a metameric reproduction under the second illuminant.

We were also interested in whether the consideration of spatial criteria in the cost function adversely affects the colorimetric accuracy of the proposed method compared with the pixel-wise PMSGM approach. For this, we computed the average CIEDE2000 color differences between the original images and the printouts (simulation) based on the proposed approach as well as the PMSGM method under the considered illuminants (CIED65 and CIEA). In Figure 10 we show the deviations between these average color differences. As can be seen, the deviations for all images are smaller than 0.2 CIEDE2000 units. For the 95th percentile of CIEDE2000 errors, the averaged difference over all considered images is -0.06 (CIED65) and 0.003 (CIEA) (a negative value indicates a higher accuracy for the proposed method, a positive value a worse accuracy). This shows that the avoidance of banding artifacts by considering spatial criterion does not come at the expense of a significant drop in colorimetric accuracy.

CONCLUSION

In this article, we proposed a methodology for spectral printing leading to almost artifact-free reproduction. Our approach takes *colorimetric* and *spatial* criteria into account and is designed to be as good as metameric reproduction for one selected illuminant (called the "most important one")

(a)   (b)   (c)   (d)
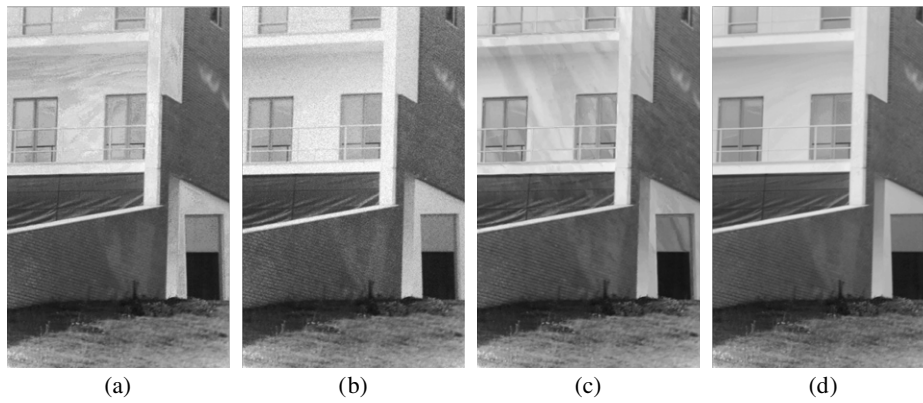
Figure 7. Separation images of a natural scene[25] (House image) generated by PMSGM[12] (a) without and (b) with the addition of a small amount of noise, (c) SGMS[13] and (d) the proposed method. It should be noted that only one channel (K) of the separation images is shown, where white = 0% ink and black = 100% ink deposition.


(a)   (b)   (c)   (d)   (e)
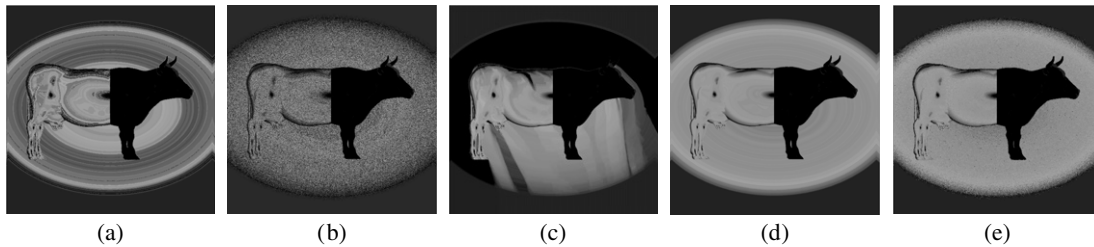
Figure 8. Separation images of a cut-out of the METACOW[18] image generated by PMSGM[12] (a) without and (b) with the addition of a small amount of noise, (c) SGMS,[13] and the proposed method (d) with additional step 1 (using two and three clusters for CIED65 and CIEA illuminants, respectively) and (e) with optional step 1 (as (d)) and optional step 2 (with the addition of a small amount of noise). It should be noted that only one channel (R) of the separation images is shown, where white = 0% ink and black = 100% ink deposition.

(a)   (b)   (c)   (d)
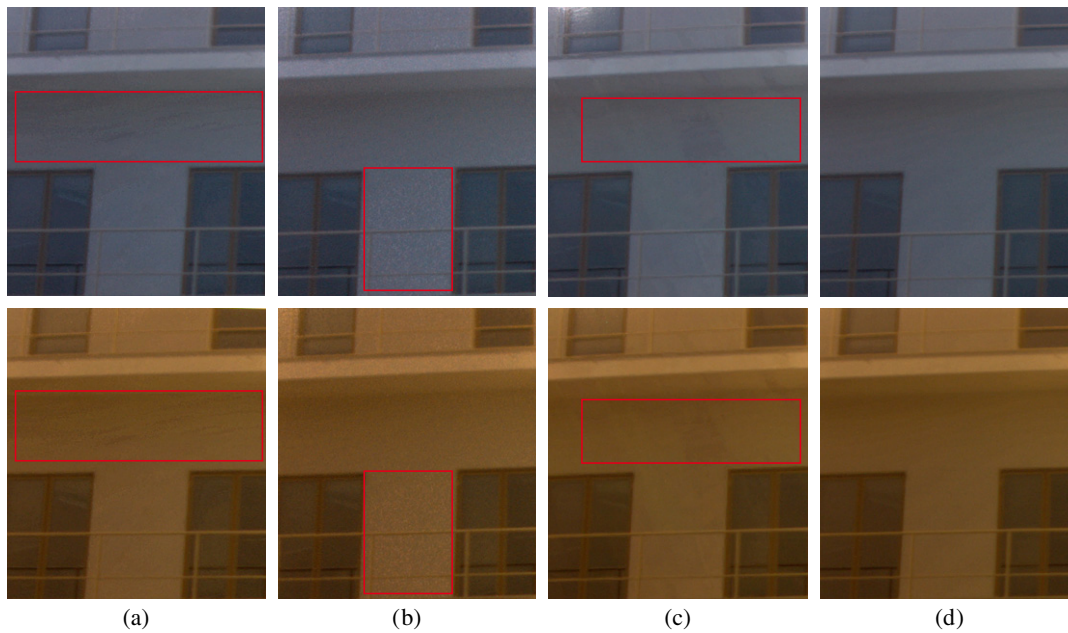
Figure 9. Cut-outs of captured images from spectral prints—based on the separations shown in Fig. 7—under the illuminants CIED65 (first row) and CIEA (second row). Different artifacts are visible in (a) (banding), (b) (graininess) and (c) (smearing), especially in the areas surrounded with red rectangles, while (d) shows the enhanced reproduction using the novel approach. It should be noted that the capture process can introduce color errors. The results are more reliable in the zoomed-in electronic version of the article.
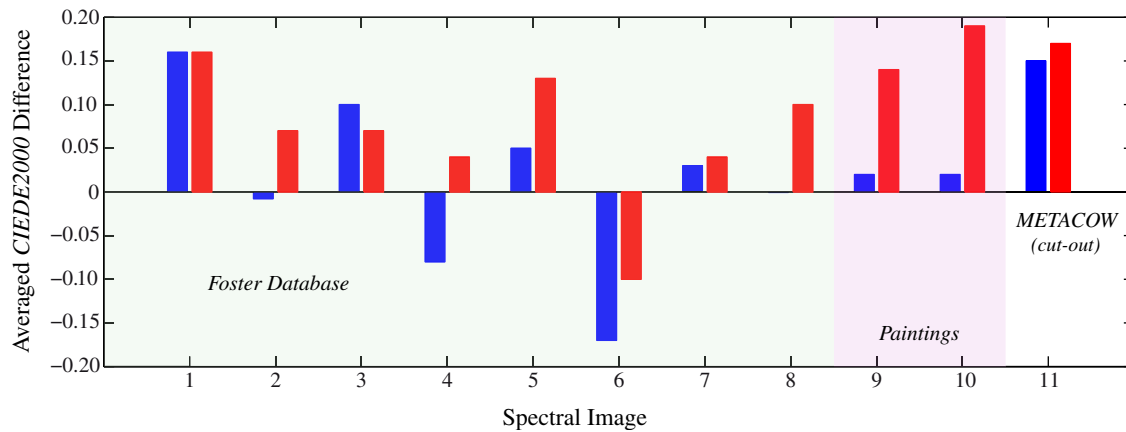
Figure 10. Deviations between average CIEDE2000 errors to the original images computed between the proposed and the PMSGM method under CIED65 (blue) and CIEA (red). Negative values indicate higher colorimetric accuracy for the proposed method, positive values worse accuracy.
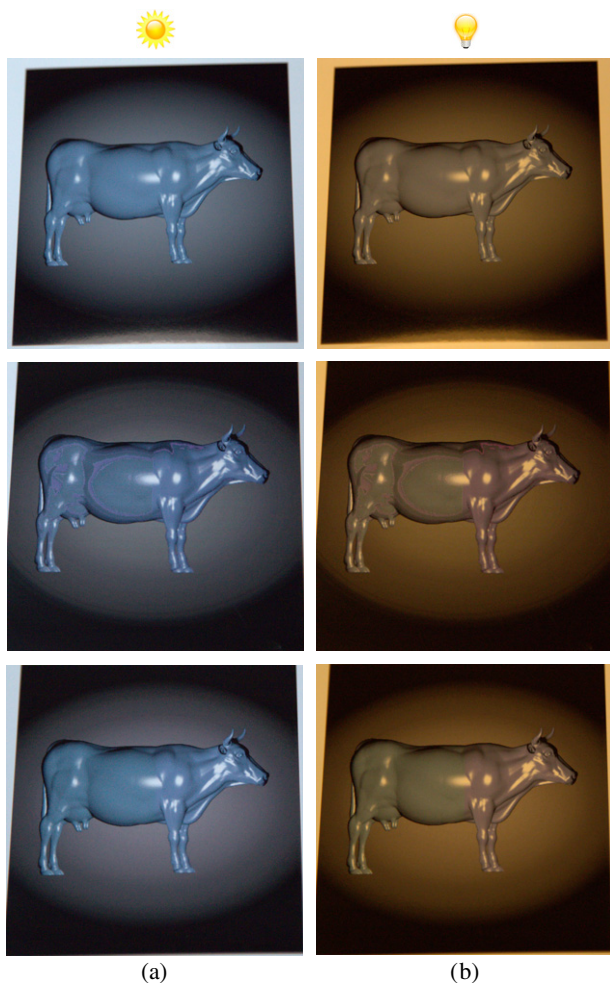
Figure 11. Captured images of real prints generated via an ICC-based metameric workflow (top row), the PMSGM approach (middle row) and the proposed method (bottom row). The capture process was performed under CIED65 (a) and CIEA (b) illuminants. It should be noted that the capture process can introduce color errors. The results are more reliable in the zoomed-in electronic version of the article.

and better for a preselected set of illuminants; a metameric gamut mapping is performed for the most important illuminant. In the next step, all pixels of the image are traversed and a gamut mapping is performed into device- and pixel-dependent paramer-mismatch gamuts. These gamuts are determined by parameric sets consisting of colorant combinations corresponding to colors within the just noticeable distance to the gamut mapped colors for the most important illuminant. In order to choose appropriate colorant combinations from these parameric sets, a cost function is minimized. This cost function has a colorimetric part for optimizing colorimetric accuracy across the considered illuminants and a spatial part for avoiding banding artifacts. A locally adaptive trade-off between the two parts ensures both high colorimetric accuracy across the considered illuminants and the avoidance of banding artifacts to a large extent for natural images. For artificial noise-free images with metameric edges, such as the METACOW[18] image, mild banding artifacts might occur. These artifacts can be fully removed by applying two additional steps: adding a small amount of noise and initializing the traversal with a clustered separation image created by a segmentation method.

We tested the proposed approach with 11 spectral images: eight natural scenes,[25] two paintings and the META-COW[18] image. The generated separation images and real spectral prints show better reproduction in terms of visible banding, graininess and smearing artifacts in comparison with results obtained by related work: PMSGM[12] and SGMS.[13] Furthermore, the colorimetric accuracy compared with the PMSGM method has not been significantly affected by considering the spatial criterion.

ACKNOWLEDGMENT

Technische Universität Darmstadt for providing the printer and required measurement equipment.

REFERENCES

[1] J. Morovic, *Color Gamut Mapping* (John Wiley & Sons, 2008).

[2] P. Urban, "Ink limitation for spectral or color constant printing," *11th Congress of the Int'l. Colour Assn.* (Sydney, Australia, 2009).

[3] D. Lau and G. Arce, *Modern Digital Halftoning*, 3rd ed. (CRC Press, 2008).

[4] D.-Y. Tzeng and R. S. Berns, "Spectral-based six-color separation minimizing metamerism," *Proc. IS&T/SID Eighth Color Imaging Conf.* (IS&T, Springfield, VA, 2000), pp. 342–347.

[5] P. Urban, M. R. Rosen, and R. S. Berns, "Fast spectral-based separation of multispectral images," *Proc. IS&T/SID, Fifteenth Color Imaging Conf.* (IS&T, Springfield, VA, 2007), pp. 178–183.

[6] M. Mahy, "Gamut Calculation of Color Reproduction Devices," *Proc. IS&T/SID Fourth Color Imaging Conf.* (IS&T, Springfield, VA, 1996), pp. 145–150.

[7] J. Morovic and M. R. Luo, "Calculating medium and image gamut boundaries for gamut mapping," Color Res. Appl. **25**, 394–401 (2000).

[8] A. M. Bakke, I. Farup, and J. Y. Hardeberg, "Multispectral gamut mapping and visualization—a first attempt," SPIE **5667**, 193–200 (2005).

[9] M. Rosen and M. Derhak, "Spectral gamuts and spectral gamut mapping," *Spectral Imaging: Eighth Int'l Symposium on Multispectral Color Science* (SPIE, San Jose, CA, 2006).

[10] S. Tsutsumi, M. R. Rosen, and R. S. Berns, "Spectral gamut mapping using LabPQR," J. Imaging Sci. Technol. **51**, no. 6, 473–485 (2007).

[11] P. Urban, M. R. Rosen, and R. S. Berns, "Spectral gamut mapping framework based on human color vision," *Proc. IS&T CGIV2008: Fourth European Conf. on Colour in Graphics, Imaging, and Vision* (IS&T, Springfield, VA, 2008), pp. 548–553.

[12] P. Urban and R. S. Berns, "Paramer mismatch-based spectral gamut mapping," IEEE Trans. Image Process. **20**, no. 6, 1599–1610 (2011).

[13] S. Samadzadegan and P. Urban, "Spatially resolved joint spectral gamut mapping and separation," *Proc. IS&T/SID, 21st Color and Imaging Conf.* (IS&T, Springfield, VA, 2013), pp. 2–7.

[14] T. Kawaguchi, N. Tsumura, H. Haneishi, M. Kouzaki, and Y. Miyake, "Vector error diffusion method for spectral color reproduction," *Proc. IS&T PICS* (IS&T, Springfield, VA, 1999), pp. 394–397.

[15] I. Lissner and P. Urban, "Toward a unified color space for perception-based image processing," IEEE Trans. Image Process. **21**, no. 3, 1153–1168 (2012).

[16] P. Zolliker and K. Simon, "Retaining local image information in gamut mapping algorithms," IEEE Trans. Image Process. **16**, no. 3, 664–672 (2007).

[17] J. Preiss, F. Fernandes, and P. Urban, "Color-image quality assessment: from prediction to optimization," IEEE Trans. Image Process. **23**, no. 3, 1366–1378 (2014).

[18] M. D. Fairchild and G. M. Johnson, "METACOW: A public-domain, high-resolution, fully-digital, noise-free, metameric, extended-dynamic-range, spectral test target for imaging system analysis and simulation," *Proc. IS&T/SID, 12th Color Imaging Conf.* (IS&T, Springfield, VA, 2004), pp. 239–245.

[19] J. A. C. Yule and W. J. Nielsen, "The penetration of light into paper and its effect on halftone reproduction," Tech. Assn. Graph. Arts **4**, 65–76 (1951).

[20] J. A. C. Yule and R. S. Colt, "Colorimetric investigations in multicolor printing," *TAGA Proc.* (1951), pp. 77–82.

[21] J. Viggiano, "The color of halftone tints," *TAGA Proc.* (1985), pp. 647–661.

[22] J. A. S. Viggiano, "Modeling the color of multi-color halftones," *TAGA Proc.* (1990), pp. 44–62.

[23] K. J. Heuberger, Z. M. Jing, and S. Persiev, "Color transformations and lookup tables," *TAGA/ISCC Proc.* (1992), pp. 863–881.

[24] A. Z. Chitade and D. S. K. Katiyar, "Colour based image segmentation using *k*-means clustering," Int. J. Eng. Sci. Technol. **2**, no. 10, 5319–5325 (2010).

[25] D. H. Foster, K. Amano, S. M. C. Nascimento, and M. Foster, "Frequency of metamerism in natural scenes," J. Opt. Soc. Am. A **23**, no. 10, 2359–2372 (2006).